

RESEARCH ARTICLE

CPVT-associated cardiac ryanodine receptor mutation G357S with reduced penetrance impairs Ca²⁺ release termination and diminishes protein expression

Yingjie Liu¹, Jinhong Wei¹, Siobhan M. Wong King Yuen², Bo Sun¹, Yijun Tang¹, Ruiwu Wang¹, Filip Van Petegem², S. R. Wayne Chen^{1*}

1 Libin Cardiovascular Institute of Alberta, Department of Physiology and Pharmacology, University of Calgary, Calgary, Alberta, Canada, **2** Department of Biochemistry and Molecular Biology, University of British Columbia, 2350 Health Sciences Mall, Vancouver, Canada

✉ Current address: Taihe Hospital Affiliated Hospital of Hubei University of Medicine, Hubei, P.R., China.
* swchen@ucalgary.ca



OPEN ACCESS

Citation: Liu Y, Wei J, Wong King Yuen SM, Sun B, Tang Y, Wang R, et al. (2017) CPVT-associated cardiac ryanodine receptor mutation G357S with reduced penetrance impairs Ca²⁺ release termination and diminishes protein expression. *PLoS ONE* 12(9): e0184177. <https://doi.org/10.1371/journal.pone.0184177>

Editor: Nicole Beard, University of Canberra, AUSTRALIA

Received: March 24, 2017

Accepted: August 18, 2017

Published: September 29, 2017

Copyright: © 2017 Liu et al. This is an open access article distributed under the terms of the [Creative Commons Attribution License](https://creativecommons.org/licenses/by/4.0/), which permits unrestricted use, distribution, and reproduction in any medium, provided the original author and source are credited.

Data Availability Statement: All relevant data are within the paper

Funding: This work was supported by research grants from the Canadian Institutes of Health Research, the Heart and Stroke Foundation of Canada, the Canada Foundation for Innovation, and the Heart and Stroke Foundation Chair in Cardiovascular Research (to S.R.W.C.). YL is a recipient of the Alberta Innovates-Health Solutions (AIHS) Studentship Award. JW is a recipient of the

Abstract

Catecholaminergic polymorphic ventricular tachycardia (CPVT) is one of the most lethal inherited cardiac arrhythmias mostly linked to cardiac ryanodine receptor (RyR2) mutations with high disease penetrance. Interestingly, a novel RyR2 mutation G357S discovered in a large family of more than 1400 individuals has reduced penetrance. The molecular basis for the incomplete disease penetrance in this family is unknown. To gain insights into the variable disease expression in this family, we determined the impact of the G357S mutation on RyR2 function and expression. We assessed spontaneous Ca²⁺ release in HEK293 cells expressing RyR2 wildtype and the G357S mutant during store Ca²⁺ overload, also known as store overload induced Ca²⁺ release (SOICR). We found that the G357S mutation reduced the percentage of RyR2-expressing cells that showed SOICR. However, in cells that displayed SOICR, G357S reduced the thresholds for the activation and termination of SOICR. Furthermore, G357S decreased the thermal stability of the N-terminal domain of RyR2, and markedly reduced the protein expression of the full-length RyR2. On the other hand, the G357S mutation did not alter the Ca²⁺ activation of [³H]ryanodine binding or the Ca²⁺ induced release of Ca²⁺ from the intracellular stores in HEK293 cells. These data indicate that the CPVT-associated G357S mutation enhances the arrhythmogenic SOICR and reduces RyR2 protein expression, which may be attributable to the incomplete penetrance of CPVT in this family.

Introduction

Catecholaminergic polymorphic ventricular tachycardia (CPVT) is an inherited, life-threatening cardiac arrhythmia characterized by stress- and emotion-induced bidirectional or polymorphic ventricular tachycardia and sudden death. Interestingly, patients susceptible to CPVT

Libin Cardiovascular Institute of Alberta and Cumming School of Medicine Postdoctoral Fellowship Award. BS is a recipient of the Heart and Stroke Foundation of Canada Junior Fellowship Award and the AIHS Fellowship Award. SRWC is an AIHS Scientist. The funders had no role in study design, data collection and analysis, decision to publish, or preparation of the manuscript.

Competing interests: The authors have declared that no competing interests exist

Abbreviations: CPVT, catecholaminergic polymorphic ventricular tachycardia; RyR2, cardiac ryanodine receptor; SR, sarcoplasmic reticulum; ER, endoplasmic reticulum; SOICR, store overload-induced Ca²⁺ release; DAD, delayed afterdepolarization; PBS, phosphate buffered saline.

generally have structurally normal hearts and normal electrocardiograph (ECG) at rest [1]. Genes encoding the cardiac ryanodine receptor (RyR2), cardiac calsequestrin (CASQ2), cardiac triadin, and calmodulin have been linked to CPVT [1–7]. Most CPVT cases are associated with mutations in RyR2 [1]. A major focus of investigation over the past decade is to understand how mutations in RyR2 cause CPVT. An increasing body of evidence indicates that CPVT is caused by delayed afterdepolarizations (DADs) and triggered activities [1, 8, 9]. DADs are the result of increased activity of the Na⁺/Ca²⁺ exchanger in response to spontaneous diastolic Ca²⁺ release from the sarcoplasmic reticulum (SR) [10–12]. Hence, spontaneous SR Ca²⁺ release is a well-known cause of CPVT.

It has long been recognized that spontaneous SR Ca²⁺ release occurs in the form of Ca²⁺ waves in cardiac cells when either the SR Ca²⁺ load exceeds a threshold level (the SR Ca²⁺ activation threshold) or the threshold is reduced to a level below the SR Ca²⁺ load [13–15]. In light of its dependence on the SR Ca²⁺ load and the SR Ca²⁺ activation threshold, we referred to this spontaneous SR Ca²⁺ release as store-overload induced Ca²⁺ release (SOICR) [1, 16, 17]. In support of the link between spontaneous SR Ca²⁺ release and CPVT, RyR2 mutations associated with CPVT were found to enhance the propensity for spontaneous Ca²⁺ release by lowering the activation threshold for SOICR [1, 8, 16–20]. Some CPVT RyR2 mutations also increased the amplitude of spontaneous Ca²⁺ release by delaying the termination of SOICR or lowering the termination threshold for SOICR [21]. Thus, these studies support the notion that the activation and termination thresholds for SOICR are important determinants of CPVT susceptibility.

CPVT is one of the most lethal cardiac arrhythmias occurring mainly in young people with sudden death often being the first symptom of CPVT patients. The mean age of onset of symptom in subjects with RyR2 mutations is ~17 years old. Furthermore, many CPVT-linked RyR2 mutations (~20%) are de novo in origin [22]. Because of the highly lethal nature of CPVT-linked RyR2 mutations, most families with CPVT RyR2 mutations are relatively small and show high penetrance (50–90%) [23–26]. Interestingly, a novel RyR2 mutation G357S has recently been discovered in a large family with 10 generations and 1404 members [27]. There are 179 G357S mutant carriers, 36 of which suffered from sudden cardiac death. Despite this lethal outcome to ~20% of the G357S positive subjects, many G357S mutant carriers lived beyond the fifth decade and even to their 70–80's [27]. This raises an important and interesting question of why the disease expression of the RyR2 mutation G357S is highly variable in this family.

The G357S mutation is located in the N-terminal region of the RyR2 channel, which consists of three individual domains: domain A (residues 1–217), domain B (residues 218–409), and domain C (residues 410–631). This region forms a tetrameric gating ring that undergoes large motions during channel opening [28–31]. Interestingly, deletion of individual domains has uncovered distinct roles in RyR2 function [32]. For instance, domain B, where the G357S mutation is located, is believed to be important for RyR2 protein expression and the activation and termination of SOICR [32]. Surprisingly, it was showed that the G357S mutation exerted little effect on the propensity for SOICR in HEK293 cells [27]. However, upon treatment with forskolin which activates PKA, the G357S-expressing HEK293 cells did display enhanced SOICR activity compared to WT expressing cells treated with forskolin [27]. These observations indicate that, unlike other N-terminal CPVT RyR2 mutations that display enhanced SOICR activity in the absence of PKA activation, the effect of the G357S mutation on SOICR requires PKA-dependent phosphorylation. It is proposed that this dependence on sympathetic activation of the effect of the G357S mutation may contribute to the reduced penetrance (28%) of CPVT in the G357S mutant carriers who may experience varied levels of sympathetic activation [27]. However, in addition to altering the response to PKA activation, it

remains to be determined whether the G357S mutation could affect other properties of the RyR2 channel.

Considering the roles of domain B in RyR2 function, in the present study, we assessed the impact of the G357S mutation on the properties of SOICR and the protein expression of RyR2. We found that although the G357S mutation had little effect on the propensity for SOICR, which is consistent with that reported previously [27], it significantly reduced the activation and termination threshold for SOICR. Furthermore, the G357S mutation decreased the thermal stability of the the N-terminal domain of RyR2, and dramatically reduced the expression of the full-length RyR2 protein. However, the G357S mutation did not alter the cytosolic Ca²⁺-dependent activation of [³H]ryanodine binding or the cytosolic Ca²⁺ regulated Ca²⁺ release in HEK293 cells. The markedly reduced protein expression of the G357S mutant may contribute to the reduced disease penetrance in this large family.

Materials and methods

Construction of the RyR2-G357S mutation

The point mutation G357S in mouse RyR2 was generated by the overlap extension method using PCR [33, 34]. Briefly, a NheI/AflII fragment with mutation G357S was obtained by overlapping PCR. The NheI/AflII fragment was removed from the PCR product and was used to replace the corresponding WT fragment in the full-length RyR2 cDNA in the expression plasmid pcDNA5. The mutation and sequence of the PCR product were confirmed by DNA sequencing.

Generation of stable inducible HEK293 cell lines and cell culture

Stable inducible HEK293 cell lines expressing RyR2 WT or the G357S mutant were generated using the Flp-In T-REx Core Kit from Invitrogen. Briefly, Flp-In T-REx-293 cells were co-transfected with the inducible expression vector pcDNA5/FRT/TO containing the RyR2 WT or mutant cDNA and the pOG44 vector encoding the Flp recombinase in 1:4 ratios using the Ca²⁺ phosphate precipitation method. The transfected cells were washed with PBS (phosphate buffered saline: 137 mM NaCl, 8 mM Na₂HPO₄, 1.5 mM KH₂PO₄ and 2.7 mM KCl, pH 7.4) 24 h after transfection followed by a change to fresh medium for 24 h. The cells were then washed again with PBS, harvested and plated onto new dishes. After the cells had attached (~4 h), the growth medium was replaced with a selection medium containing 200 µg/ml hygromycin (Invitrogen). The selection medium was changed every 3–4 days until the desired number of cells was grown. The hygromycin-resistant cells were pooled, aliquoted (1 ml) and stored at –80°C. These positive cells are believed to be isogenic because the integration of RyR2 cDNA is mediated by the Flp recombinase at a single FRT site. HEK293 cells were maintained in Dulbecco's modified Eagle's medium (DMEM) supplemented with 0.1 mM minimum Eagle's medium nonessential amino acids, 4 mM L-glutamine, 100 units of penicillin / ml, 100 mg of streptomycin/ml, 4.5 g of glucose/ liter, and 10% fetal calf serum, at 37 °C under 5% CO₂.

Immunoblotting

HEK293 cell lines grown for 24 h after induction by 1 µg/ml tetracycline (Sigma) were washed with PBS plus 2.5 mM EDTA and harvested in the same solution by centrifugation for 8 min at 700 g in an IEC Centra-CL2 centrifuge. The cells were then washed with PBS without EDTA and centrifuged again at 700 g for 8 min. The PBS-washed cells were solubilized in a lysis buffer containing 25 mM Tris, 50 mM Hepes (pH 7.4), 137 mM NaCl, 1% CHAPS, 0.5% soya bean phosphatidylcholine, 2.5 mM DTT and a protease inhibitor mix (1 mM benzamidine,

2 µg/ml leupeptin, 2 µg/ml pepstatin A, 2 µg/ml aprotinin and 0.5 mM PMSF). This mixture was incubated on ice for 1 h. Cell lysates were obtained by centrifuging twice at 16000 g in a microcentrifuge at 4°C for 30 min to remove unsolubilized materials. The RyR2 WT and G357S mutant proteins were subjected to SDS/PAGE (6% gel) and transferred onto nitrocellulose membranes at 100 V for 2 h at 4°C in the presence of 0.01% SDS [35, 36]. The nitrocellulose membranes containing the transferred proteins were blocked for 45 min with 1x PBS and 1% Casein Blocker (Bio-Rad). The blocked membrane was incubated with the anti-RyR antibody (34C) (Thermo Scientific, MA3-925, 1:1000 dilution) and then incubated with the secondary anti-[mouse IgG (heavy and light)] antibodies conjugated to horseradish peroxidase (1:20,000 dilution). For β-actin determination, the blocked membrane was incubated with the anti-β-actin antibody (1:5000) and then incubated with the same secondary antibody. After washing for 5 min three times, the bound antibodies were detected using an enhanced chemiluminescence kit from Pierce.

Single-cell cytosolic Ca²⁺ imaging of HEK293 cells

Cytosolic Ca²⁺ levels in stable inducible HEK293 cells expressing RyR2 WT or G357S were monitored using single cell Ca²⁺ imaging and the fluorescent Ca²⁺ indicator dye Fura-2 AM (Fura-2 acetoxyethyl ester) as described previously [16, 17]. Briefly, cells grown on glass coverslips for 18–22 h after induction by 1 µg/ml tetracycline were loaded with 5 µM Fura-2 AM in KRH (Krebs–Ringer–Hepes) buffer (125 mM NaCl, 5 mM KCl, 1.2 mM KH₂PO₄, 6 mM glucose, 1.2 mM MgCl₂ and 25 mM Hepes, pH 7.4) plus 0.02% pluronic F-127 and 0.1 mg/ml BSA for 20 min at room temperature (23°C). The coverslips were then mounted in a perfusion chamber (Warner Instruments) on an inverted microscope (Nikon TE2000-S). The cells were perfused continuously with KRH buffer containing increasing extracellular Ca²⁺ concentrations (0, 0.1, 0.2, 0.3, 0.5, 1.0, and 2.0 mM). Caffeine (10 mM) was applied at the end of each experiment to confirm the expression of active RyR2 channels. Time-lapse images (0.25 frame/s) were captured and analyzed with Compix Simple PCI 6 software. Fluorescence intensities were measured from regions of interest centered on individual cells. Only cells that responded to caffeine were analyzed. The filters used for Fura 2 imaging were λ_{ex} = 340 ± 26 nm and 387 ± 11 nm, and λ_{em} = 510 ± 84 nm with a dichroic mirror (410 nm).

Single-cell luminal Ca²⁺ imaging of HEK293 cells

Luminal Ca²⁺ levels in HEK293 cells expressing RyR2-WT or G357S were measured using single-cell Ca²⁺ imaging and the FRET (fluorescence resonance energy transfer)-based ER luminal Ca²⁺-sensitive cameleon protein D1ER as described previously [19, 37]. The cells were grown to 95% confluence in a 75 cm² flask, passaged with PBS and plated in 100-mm-diameter tissue culture dishes at ~40% confluence 18–20 h before transfection with D1ER cDNA using the calcium phosphate precipitation method. After transfection for 24 h, the growth medium was then changed to an induction medium containing 1 µg/ml tetracycline (Sigma). After induction for ~22 h, the cells were perfused continuously with KRH buffer containing various concentrations of Ca²⁺ (0, 1 and 2 mM) and tetracaine (1 mM) for estimating the store capacity or caffeine (20 mM) for estimating the minimum store level by depleting the ER Ca²⁺ stores at room temperature (23°C). In permeabilized cells studies, the cells were first permeabilized with 50 µg/ml saponin in an incomplete intracellular-like medium (125 mM KCl, 19 mM NaCl, and 10 mM HEPES, pH 7.4 with KOH) at room temperature (23°C) for 3–4 min [38]. The cells were then switched to a complete intracellular-like medium (incomplete intracellular-like medium plus 2 mM ATP, 2 mM MgCl₂, 0.05 mM EGTA, and 100 nM free Ca²⁺, pH 7.4 with KOH) for 5–6 min to remove saponin. The permeabilized cells were then perfused with

various concentrations of Ca²⁺ (0.1, 0.2, 0.4, 1, and 10 μ M) followed by tetracaine (1 mM) for estimating the store capacity and caffeine (20 mM) for estimating the minimum store level by depleting the ER Ca²⁺ stores. Images were captured with Compix Simple PCI 6 software every 2s using an inverted microscope (Nikon TE2000-S) equipped with an S-Fluor 20 \times /0.75 objective. The filters used for DIER imaging were $\lambda_{ex} = 436\pm 20$ nm for CFP and $\lambda_{ex} = 500\pm 20$ nm for YFP, and $\lambda_{em} = 465\pm 30$ nm for CFP and $\lambda_{em} = 535\pm 30$ nm for YFP with a dichroic mirror (500 nm). The amount of FRET was determined from the ratio of the light emission at 535 and 465 nm.

[³H]Ryanodine binding

HEK293 cell lines grown for 24 h after induction by 1 μ g/ml tetracycline (Sigma) were washed with PBS plus 2.5 mM EDTA and harvested in the same solution by centrifugation for 8 min at 700 g in an IEC Centra-CL2 centrifuge. The cells were then washed with PBS without EDTA and centrifuged again at 700 g for 8 min. The PBS-washed cells were solubilized in a lysis buffer containing 25 mM Tris, 50 mM Hepes (pH 7.4), 137 mM NaCl, 1% CHAPS, 0.5% soya bean phosphatidylcholine, 2.5 mM DTT and a protease inhibitor mix (1 mM benzamide, 2 μ g/ml leupeptin, 2 μ g/ml pepstatin A, 2 μ g/ml aprotinin and 0.5 mM PMSF). This mixture was incubated on ice for 1 h. Cell lysates were obtained by centrifuging twice at 16000 g in a microcentrifuge at 4°C for 30 min to remove unsolubilized materials. Equilibrium [³H]ryanodine binding to cell lysates was performed as described previously [39] with some modifications. [³H]Ryanodine binding was carried out in a total volume of 300 μ l binding solution containing 30 μ l of cell lysate, 500 mM KCl, 25 mM Tris, 50 mM Hepes (pH 7.4), 5 nM [³H] ryanodine and CaCl₂ to set free [Ca²⁺] from pCa 9.89 to pCa 4 and a protease inhibitor mix at 37°C for 20 min. The Ca²⁺/EGTA ratio was calculated using the computer program described by Fabiato and Fabiato [40]. The binding mix was diluted with 5 ml of ice-cold washing buffer containing 25 mM Tris/HCl, pH 8.0, and 250 mM KCl and immediately filtered through Whatman GF/B filters presoaked with 1% polyethyleneimine. The filters were washed three times, and the radioactivity associated with the filters was determined by liquid scintillation counting. Non-specific binding was determined by measuring [³H]ryanodine binding in the presence of 50 μ M unlabelled ryanodine. Maximum [³H]ryanodine binding was determined by measuring binding in the presence of 100 μ M free Ca²⁺, 2.5 mM ATP, and 2.5 mM caffeine. All binding assays were performed in duplicate.

Expression and purification of the N-terminal RyR2ABC mutant protein

Mouse RyR2 (residues 1–547 = RyR2ABC), harboring the G357S mutation, was purified using similar procedures as described before for WT RyR2ABC [41]. In brief, the protein was expressed in the E. coli Rosetta strain as a fusion protein containing an N-terminal His-tag, maltose binding protein, and a cleavage site for Tobacco Etch Virus (TEV) Protease. After affinity steps using Nickel and amylose resin, the tag was removed with recombinant TEV protease, and further purified using Nickel, anion exchange, and size exclusion chromatography.

Thermal melt assays

Reaction mixtures consisting of a final protein concentration of 0.3 mg/mL (in 150 mM KCl, 10 mM HEPES, pH 7.4) and a 5,000x dilution of SYPRO® Orange Protein Gel Stain (Life Technologies) were assembled in MicroAmp® Fast Optical 48-well reaction plates (Applied Biosystems) and sealed with optical adhesive covers (Applied Biosystems). The plate was placed into a StepOnePlus Real Time PCR System (Applied Biosystems) and heated from 25°C to 95°C with a change in temperature of 0.5°C per cycle. For each construct, three replicates

were performed. The resulting data were normalized, averaged and graphed using GraphPad Prism5. The first derivatives were generated to calculate the melting temperatures. Statistical significance was determined using an unpaired two-tailed t-test with a 95% confidence level.

Statistical analysis

All values shown are mean \pm SEM unless indicated otherwise. To test for differences between groups, we used Student's *t*-test (2-tailed). A *P* value <0.05 was considered to be statistically significant.

Results

Effect of the CPVT-associated RyR2 G357S mutation on the propensity for store-overload induced Ca²⁺ release (SOICR)

We have previously shown that CPVT-associated RyR2 mutations enhance the propensity for store Ca²⁺ overload-induced spontaneous Ca²⁺ release (SOICR) in HEK293 cells [1, 16, 17, 19]. To assess the effect of the CPVT-associated RyR2 G357S mutation on SOICR, we generated stable, inducible HEK293 cell lines expressing RyR2 WT or the RyR2 G357S mutant. The WT or G357S mutant expressing HEK293 cells were perfused with increasing concentrations of extracellular Ca²⁺ (0–2 mM) to induce SOICR as described previously [16, 17]. The SOICR activity was then monitored by using the fluorescence Ca²⁺ dye Fura-2 AM and single cell Ca²⁺ imaging. The number of HEK293 cells that displayed spontaneous Ca²⁺ oscillations at each extracellular Ca²⁺ concentration was determined and normalized to the total number of cells that responded to caffeine (10 mM) to obtain the fraction of oscillating cells for each condition. The increase in the fraction of oscillating cells in response to elevated extracellular Ca²⁺ concentrations reflects the propensity for SOICR. As shown in Fig 1, WT and G357S-expressing HEK293 cells showed similar fractions of oscillating cells at low extracellular Ca²⁺ concentrations (0–0.3 mM). However, the G357S mutant expressing HEK293 cells showed reduced fractions of oscillating cells at higher extracellular Ca²⁺ concentrations (0.5–2 mM) as compared with WT-expressing HEK293 cells. At 2 mM extracellular Ca²⁺, the fraction of oscillating G357S cells is $47.5 \pm 2.5\%$, significantly lower than that of oscillating WT cells ($65.3 \pm 4.0\%$). Hence, unlike most of the CPVT-associated RyR2 mutations, the G357S mutation reduces the maximum fraction of HEK293 cells that show SOICR, but does not appear to enhance the propensity for SOICR in HEK293 cells at low extracellular Ca²⁺ concentrations.

The G357S mutation decreases both the activation and termination thresholds for SOICR

To further study the effect of the G357S mutation on the properties of SOICR in HEK293 cells that show SOICR, we monitored the endoplasmic reticulum (ER) Ca²⁺ dynamics using a FRET-based ER luminal Ca²⁺-sensing probe D1ER [19, 37]. As shown in Fig 2, increasing extracellular Ca²⁺ concentration from 0 to 2 mM induced spontaneous ER Ca²⁺ oscillations in RyR2 expressing HEK293 cells, shown as downward deflections in D1ER signal. SOICR occurred when ER luminal Ca²⁺ reaches the activation threshold level (F_{SOICR}) and terminated when ER luminal Ca²⁺ decreased to the termination threshold level (F_{termi}). The activation and termination thresholds were calculated as described in Fig 2A, and the fractional Ca²⁺ release (activation threshold–termination threshold) represents the fraction of Ca²⁺ release during SOICR. The G357S mutation significantly reduced the activation threshold (G357S: $90.1 \pm 0.4\%$ vs. WT: $93.2 \pm 0.3\%$) ($P < 0.01$) and the termination threshold (G357S: $50.4 \pm 1.3\%$ vs. WT: $58.8 \pm 0.9\%$) ($P < 0.01$) (Fig 2B, 2C and 2D). The G357S mutation also resulted in an

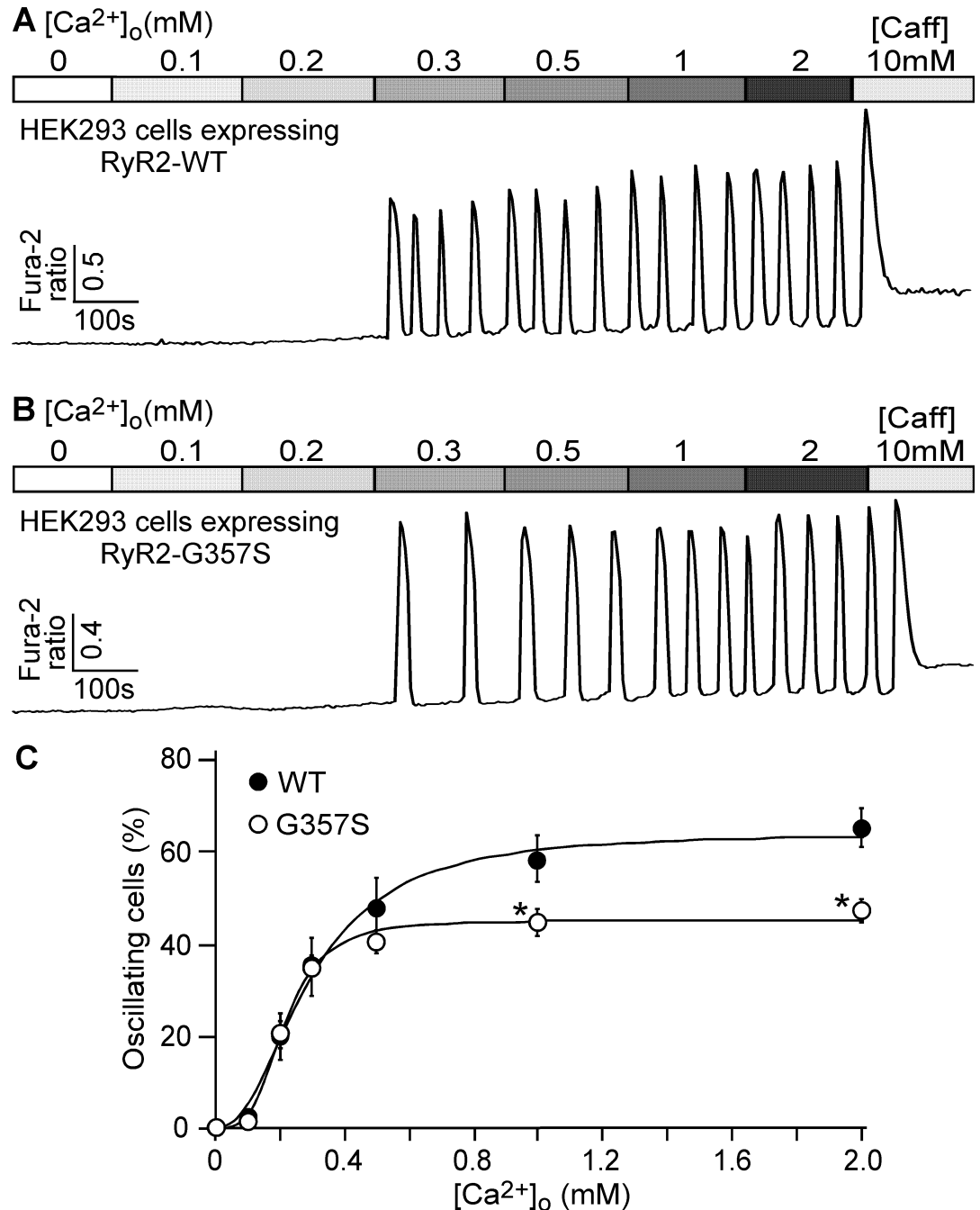


Fig 1. Effect of the CPVT-associated RyR2 G357S mutation on the propensity for store overload-induced Ca²⁺ release (SOICR). Stable, inducible HEK-293 cells expressing RyR2 WT (A) or RyR2 G357S (B) were loaded with 5μM Fura-2 AM in KRH buffer. The cells were then perfused continuously with KRH buffer containing increasing levels of extracellular Ca²⁺ (0–2 mM) to induce SOICR. Fura-2 ratios were recorded using epifluorescence single cell Ca²⁺ imaging. C, the percentage of RyR2 WT (898 cells) and the G357S mutant (846 cells) cells that displayed Ca²⁺ oscillations at various extracellular Ca²⁺ concentrations (n = 7). Data shown are mean ± SEM (*, p<0.01 vs WT; NS, not significant).

<https://doi.org/10.1371/journal.pone.0184177.g001>

increased fractional Ca²⁺ release (G357S: 39.7 ± 1.0% vs. WT: 34.4 ± 0.8%) (P<0.01)(Fig 2E). The store capacity of ER luminal Ca²⁺ (F_{max}-F_{min}) was not significantly different between WT

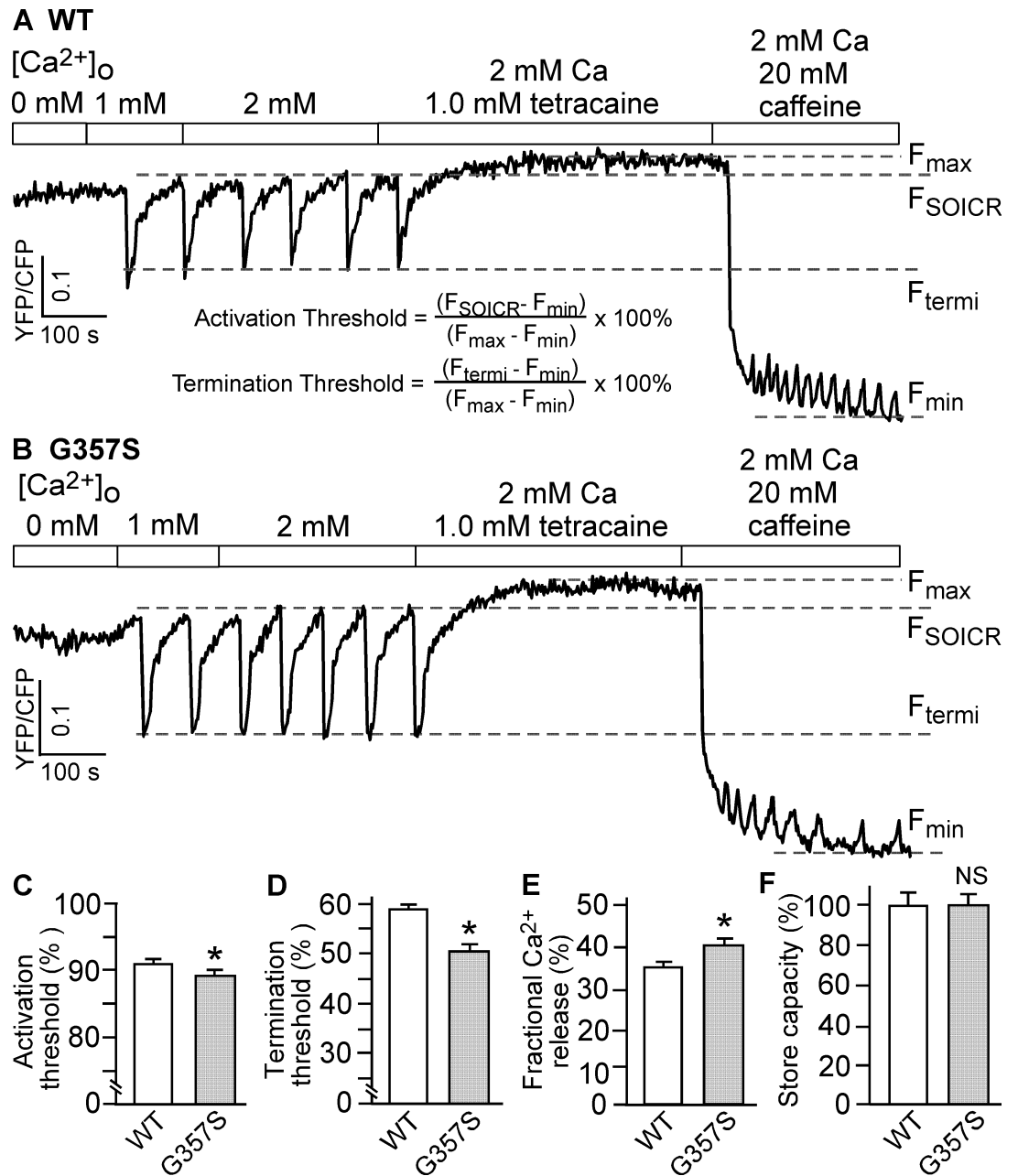


Fig 2. The G357S mutation decreases both activation and termination thresholds for SOICR. Stable, inducible HEK293 cell lines expressing RyR2 WT (A) or the G357S mutant (B) were transfected with the FRET-based ER luminal Ca²⁺-sensing protein D1ER and induced using tetracycline before the experiment. The cells were perfused with KRH buffer containing increasing levels of extracellular Ca²⁺ (0–2 mM) to induce SOICR. FRET recordings from representative cells (total 72 for WT and 77 for G357S) are shown. To minimize the influence by YFP/CFP cross-talk, we used relative FRET measurements for calculating the activation threshold (C) and termination threshold (D) using the equations shown in A. F_{SOICR} indicates the FRET level at which SOICR occurs, whereas F_{termi} represents the FRET level at which SOICR terminates. The fractional Ca²⁺ release (E) was calculated by subtracting the termination threshold from the activation threshold. The maximum FRET signal F_{max} is defined as the FRET level after tetracaine treatment. The minimum FRET signal F_{min} is defined as the FRET level after caffeine treatment. The store capacity (F) was calculated by subtracting F_{min} from F_{max}. Data shown are mean ± SEM (n = 5–6) (*, p < 0.01 vs WT; NS, not significant).

<https://doi.org/10.1371/journal.pone.0184177.g002>

and G357S (Fig 2F) ($P > 0.1$). Furthermore, SOICR did not occur in control HEK293 cells expressing no RyR2, and that SOICR was not affected by the IP3R inhibitor, xestospongin C [21], indicating that SOICR is mediated by RyR2. These data indicate that the G357S mutation enhances the susceptibility to spontaneous Ca²⁺ release by reducing the SOICR activation threshold, and augments the amplitude of spontaneous Ca²⁺ release by increasing the fractional Ca²⁺ release as a result of delayed SOICR termination.

The G357S mutation markedly reduces the level of RyR2 expression in HEK293 cells

Since the occurrence of SOICR in HEK293 cells depends on the expression of RyR2 [21], the reduced fraction of oscillating cells observed in G357S-expressing HEK293 cells may result from impaired expression of the G357S mutant. To test this possibility, we performed immunoblotting analysis using an anti-RyR antibody to compare the protein levels of WT and the G357S mutant expressed in HEK293 cells. As shown in Fig 3, the expression level of RyR2 in G357S-expressing HEK293 cells is $33.6 \pm 1.8\%$ of that in RyR2 WT-expressing cells (Fig 3A and 3B). Since ryanodine only binds to the open conformation of RyRs, [³H]ryanodine

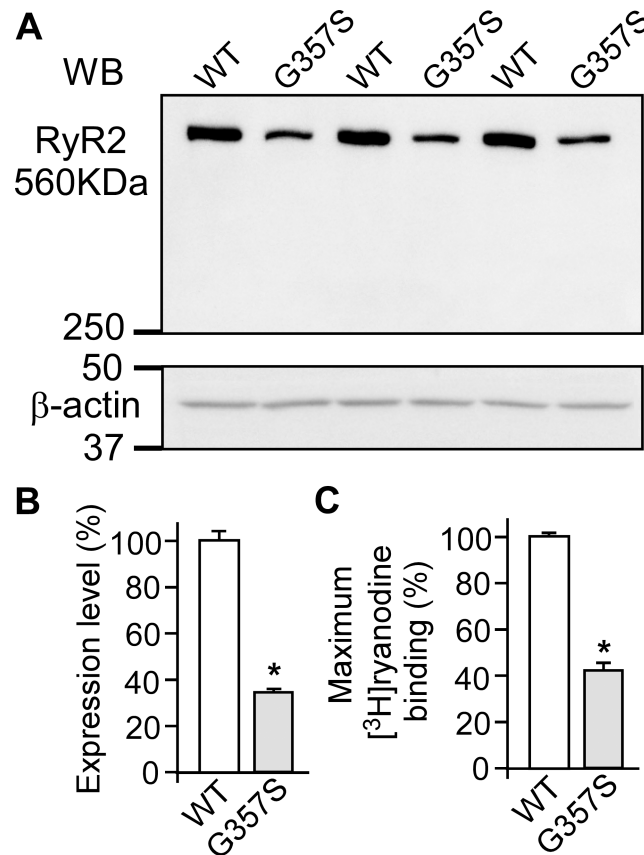


Fig 3. The G357S mutation markedly reduces the level of RyR2 expression in HEK293 cells. Stable, inducible HEK293 cells expressing RyR2 WT or the G357S mutant were collected and lysed after induction for 24 h. The same amount of HEK293 cell lysate protein was used for Western blotting (WB) (A, B) using the anti-RyR antibody (34c) and anti-β-actin antibody or for [³H]ryanodine binding in the presence of 500 mM KCl, 5 nM [³H]ryanodine, 100 μM Ca²⁺, 2.5 mM ATP, and 2.5 mM caffeine (C). The expression level and the maximum [³H]ryanodine binding of the G357S mutant was normalized to that of RyR2 WT. Data shown are mean ± SEM (n = 3) (*, p < 0.05 vs WT).

<https://doi.org/10.1371/journal.pone.0184177.g003>

binding has widely been used for monitoring the activity of the RyR channel. Therefore, we also carried out [³H]ryanodine binding to lysates of RyR2 WT and G357S mutant cells to estimate the expression levels of functional WT and the G357S mutant protein. Consistent with the immunoblotting analysis, the maximum [³H]ryanodine binding (in the presence of 100 μM Ca²⁺, 2.5 mM ATP and 2.5 mM caffeine) to the G357S mutant cell lysate is 42.5 ± 2.7% of that to the WT cell lysate (Fig 3C). These data demonstrate that the G357S mutation substantially decreases the expression level of the RyR2 protein.

The G357S mutation does not affect cytosolic Ca²⁺-dependent activation of [³H]ryanodine binding

Our previous studies showed that depending on their locations, some CPVT-associated RyR2 mutations enhance the Ca²⁺ dependent activation of [³H]ryanodine binding, while other CPVT-associated RyR2 mutations do not [16, 17]. To assess whether the G357S mutation alters the Ca²⁺ dependence of [³H]ryanodine binding, we performed [³H]ryanodine binding to WT and the G357S mutant in the presence of a wide range of Ca²⁺ concentrations. As shown in Fig 4, the cytosolic Ca²⁺ dependence of [³H]ryanodine binding to the WT and G357S mutant was indistinguishable with an EC50 value of 0.21 ± 0.01 μM for WT and 0.20 ± 0.01 μM for G357S (P > 0.1) (Fig 4A). Consistent with those shown in Fig 3, the maximum [³H]ryanodine binding to the G357S mutant was significantly reduced as compared with the maximum [³H]ryanodine binding to the RyR2-WT (Fig 4B). These data suggest that the G357S mutation does not affect the cytosolic Ca²⁺-dependent activation of RyR2.

The G357S mutation has little effect on cytosolic Ca²⁺-regulated Ca²⁺ release in HEK293 cells

To assess the effect of the G357S mutation on the Ca²⁺ dependent activation of RyR2 in a cellular environment, we determined the level of Ca²⁺ release in permeabilized HEK293 cells triggered by various cytosolic Ca²⁺ concentrations. HEK293 cells expressing the RyR2 WT and G357S mutant were first permeabilized to allow access to cytosolic Ca²⁺. Permeabilized cells were then perfused with various cytosolic Ca²⁺ concentrations (0.1–10 μM). The fractional Ca²⁺ release induced by various cytosolic Ca²⁺ concentrations was monitored by measuring the steady-state ER Ca²⁺ level as described previously [19, 37, 38]. As shown in Fig 5, increasing cytosolic Ca²⁺ concentrations from 0.1 to 10 μM reduced the steady state ER Ca²⁺ level in permeabilized HEK293 cells expressing RyR2 WT (Fig 5A and 5F), which reflects cytosolic Ca²⁺ induced fractional Ca²⁺ release from the ER Ca²⁺ store. The steady state ER Ca²⁺ level at each cytosolic Ca²⁺ concentration in the G357S mutant expressing HEK293 cells is indistinguishable from that in WT-expressing cells. Thus, consistent with the [³H]ryanodine binding data, the G357S mutation does not affect the cytosolic Ca²⁺ dependent activation of RyR2.

The G357S mutation reduces the stability of the N-terminal region of RyR2

Since the G357S mutation reduces RyR2 protein expression (Fig 3), we wondered whether this effect is intrinsic to the N-terminal region where the mutation is located. We expressed the N-terminal region of RyR2 (RyR2ABC) containing the G357S mutation as a fusion protein with His-tag and maltose binding protein (MBP), removed the tags and purified it to homogeneity (Fig 6A and 6B). Fig 6C shows thermal melting curves using a ThermoFluor. There are two transitions in the thermal melt for the G357S mutant with the first transition exhibiting a melting temperature significantly lower than that of the RyR2ABC-WT (RyR2ABC-G357S):

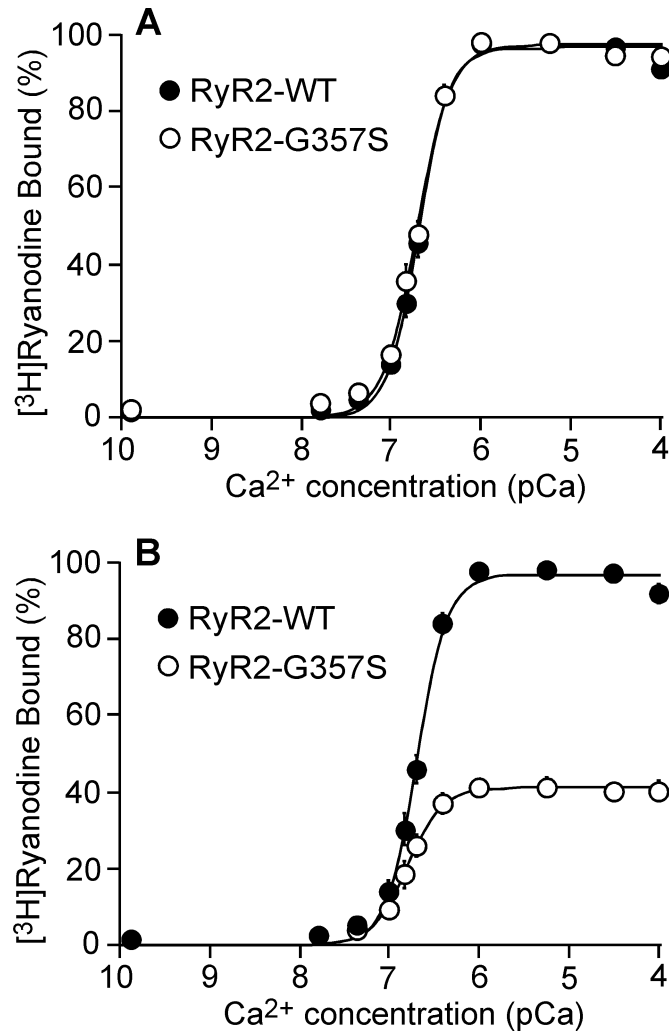


Fig 4. The G357S mutation does not affect cytosolic Ca²⁺ dependent activation of [3H]ryanodine binding. [3H]ryanodine binding to cell lysates prepared from HEK293 cells expressing RyR2 WT or the G357S mutant was carried out at various Ca²⁺ concentrations (~0.2 nM-0.1 mM), 500 mM KCl and 5 nM [3H] ryanodine. (A) [3H]ryanodine bound to RyR2 WT or G357S at various Ca²⁺ concentrations was normalized to its own maximal binding (100%). (B) [3H]ryanodine bound at various Ca²⁺ concentrations was normalized to the maximal binding to RyR2 WT (100%). The data points shown are mean ± SEM from three separate experiments.

<https://doi.org/10.1371/journal.pone.0184177.g004>

39.8 ± 0.17°C vs RyR2ABC-WT: 42.8 ± 0.17°C, P = 0.0002). These results indicate that the G357S mutation has an intrinsically destabilizing effect on the RyR2ABC. In the context of the full-length RyR2, the G357S mutation is close to an interface with the Central domain that encompasses disease hot spot 3 [1, 42, 43] (Fig 6E). Within the individual RyR2ABC domains, G357 is exposed to the surface, and the introduction of a serine side chain would not cause any steric clash with another side chain (Fig 6A and 6B). This may seem at odds with the dramatically reduced expression of the RyR2 protein, but a closer inspection of the backbone dihedral angles explains this. Because of the absence of a C-beta atom, glycine residues can adopt conformations that are not allowed for other amino acids. Fig 6D shows a Ramachandran plot for the RyR2ABC WT protein (PDB code 4L4H). The G357 residue is located in the middle of a disallowed region for non-glycine residues. Substitution by serine would thus cause an

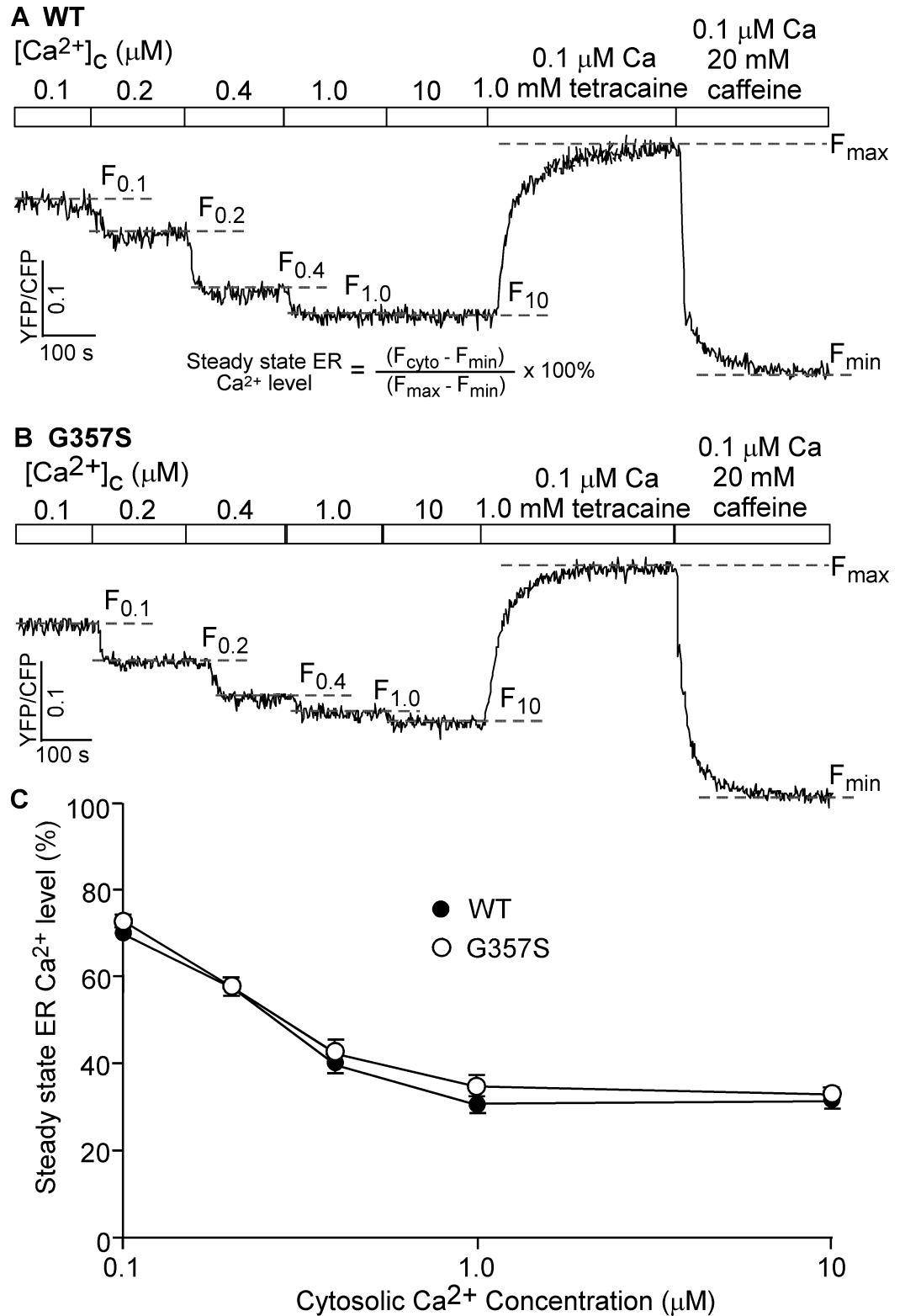


Fig 5. The G357S mutation has little effect on cytosolic Ca²⁺-regulated Ca²⁺ release. Stable, inducible HEK293 cell lines expressing RyR2 WT (A) or G357S (B) were transfected with the FRET-based ER luminal Ca²⁺-sensing protein D1ER and induced using tetracycline. The transfected and induced cells were permeabilized with saponin, washed, and perfused with intracellular-like medium plus increasing levels of free Ca²⁺ (0.1, 0.2, 0.4, 1 and 10 μM).

FRET recordings from representative cells (total 89 for WT and 87 for G357S) are shown. To minimize the influence by YFP/CFP cross-talk, we used relative FRET measurements for calculating the steady state ER Ca²⁺ level (defined in A) (C). The dashed lines ($F_{0.1}$ - F_{10}) indicate the steady state FRET levels after perfusing with each Ca²⁺ concentration (0.1, 0.2, 0.4, 1, or 10 μ M). The maximum FRET signal F_{max} is defined as the FRET level after tetracaine treatment. The minimum FRET signal F_{min} is defined as the FRET level after caffeine treatment. The store capacity (D) was calculated by subtracting F_{min} from F_{max} . Data shown are mean \pm SEM (n = 4–6).

<https://doi.org/10.1371/journal.pone.0184177.g005>

intrinsic destabilization of the protein, and we postulate that this underlies the effect on the stability of the G357S mutant protein.

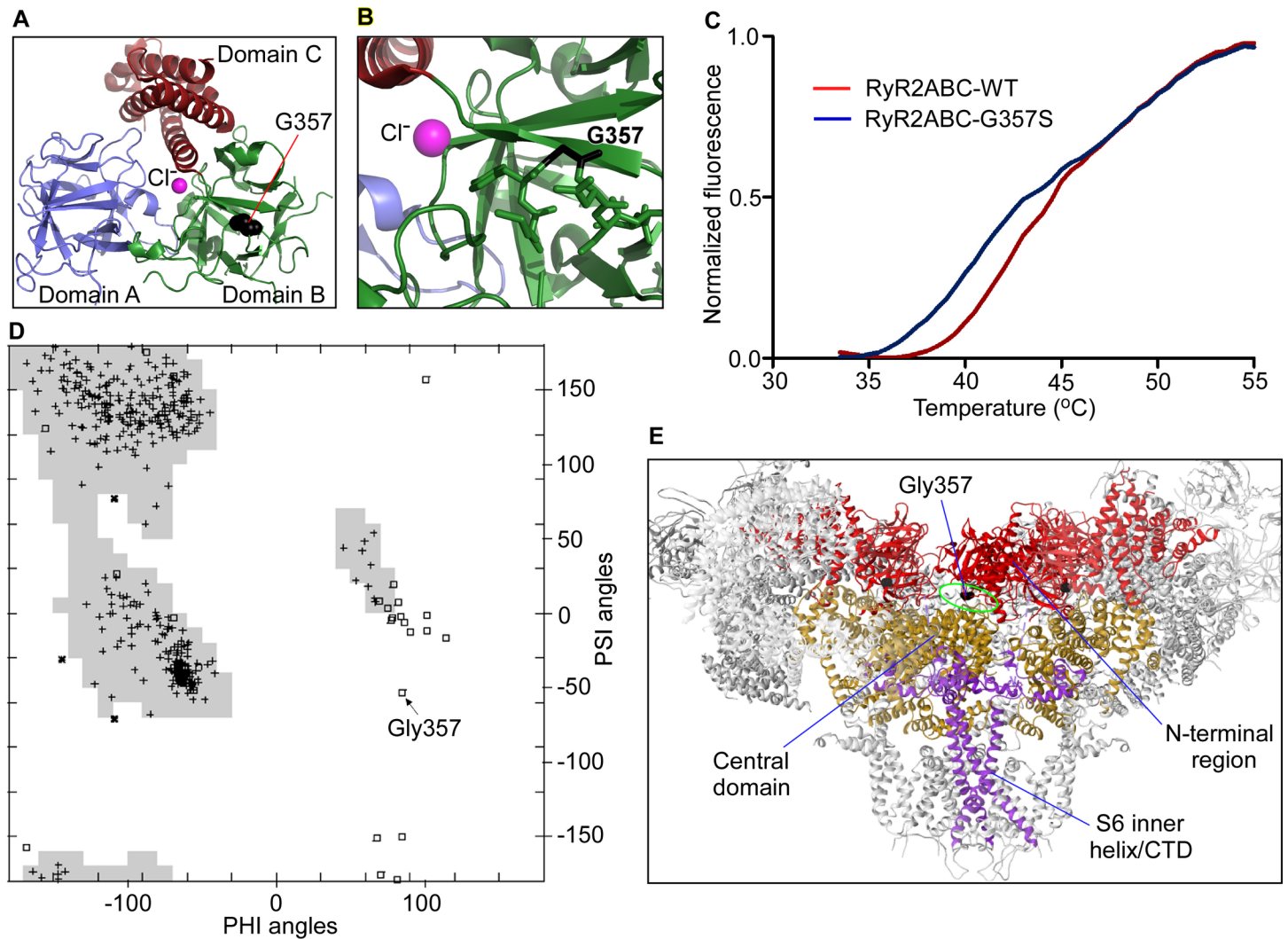


Fig 6. The G357S mutation reduces the stability of the ABC domains of RyR2. **A.** Crystal structure of the mouse RyR2ABC (residues 1–547), showing three domains and a central chloride anion that links the three domains together. **B.** Details showing G357S. The backbone conformation is allowed for glycine, but not serine. **C.** Thermal melting curves indicating thermal stability of WT RyR2ABC vs. G357S RyR2ABC. The melting temperatures, obtained by taking the maxima of the first derivatives, are $42.8^{\circ}\text{C} \pm 0.17^{\circ}\text{C}$ for RyR2ABC WT and $39.8^{\circ}\text{C} \pm 0.17^{\circ}\text{C}$ for RyR2ABC G357S (errors indicating SEM). Statistical significance was determined using an unpaired two-tailed t-test with a 95% confidence level, with $P = 0.0002$. **D.** Ramachandran plot for the RyR2ABC crystal structure, with backbone phi angles on the X-axis, and psi angles on the Y-axis. The shaded areas indicate preferred regions for non-glycine residues. Glycine residues are indicated with squares, with G357 indicated by an arrow. **E.** Cryo-EM structure of RyR [42, 43], showing the location of the corresponding glycine. One subunit, at the 'front' of the viewer, has been left out for clarity. The N-terminal region, the Central domains, and the S6 inner helix bundle with the COOH-terminal domain (CTD) are indicated. The equivalent of G357 in RyR1 is near the interface between the N-terminal region and the Central domain.

<https://doi.org/10.1371/journal.pone.0184177.g006>

Discussion

Catecholaminergic polymorphic ventricular tachycardia (CPVT) is thought to be one of the most lethal forms of inherited ion channelopathies [22, 26, 44–47]. However, not all CPVT patients experience this highly lethal phenotypes. Recently, Wangüemert et al. [27] described a large family of more than 1400 members with multiple cases of CPVT and sudden cardiac death. Surprisingly, many G357S mutant carriers lived beyond the age of 50 and some even to their 70–80's. The mechanism underlying this variable phenotypic expression is unknown.

Understanding the molecular and cellular defects of the RyR2 G357S mutation may provide some clues to the reduced penetrance of CPVT in this large family. Wangüemert et al. [27] showed that the functional impact of the G357S mutation requires sympathetic activation, and suggested that this dependence on beta-adrenergic stimulation may underlie the incomplete penetrance of the disease in this family. In the present study, we determined the impact of the G357S mutation on RyR2 function and expression. We found that the N-terminal G357S mutation reduces the activation and termination thresholds for the arrhythmogenic spontaneous Ca²⁺ release (SOICR), similar to the impact of other N-terminal CPVT RyR2 mutations characterized previously [17, 21]. However, unlike other N-terminal CPVT RyR2 mutations, the G357S mutation also substantially decreases the expression level of the RyR2 protein. These effects of the G357S mutation on SOICR thresholds and protein expression likely contribute to the variable disease phenotypes observed in this family.

It is well established that spontaneous Ca²⁺ release (SOICR) can lead to DADs and triggered activity, which is a major cause of CPVT [1, 8–12]. Hence, a reduced threshold for SOICR activation will enhance the occurrence of SOICR. Furthermore, a reduced threshold for SOICR termination (or a delayed termination) will increase the fractional SR Ca²⁺ release or the amplitude of SOICR. The increased occurrence and amplitude of SOICR would, in turn, increase the amplitude of DADs and thus the propensity for triggered activity and CPVT. Therefore, the enhanced SOICR activity as a result of the G357S mutation may explain the lethal CPVT phenotypes observed in some of the mutant carriers in this large family.

A functional RyR2 channel consists of 4 subunits that form a tetrameric structure. In patients heterozygous for the G357S mutation, the RyR2 channel is composed of both the WT and G357S mutant. The impact of the mutant on RyR2 function would depend on the ratio of the WT and mutant, which depends on the level of expression of the WT and mutant alleles. In the present study, we found that the G357S mutation substantially reduces the level of expression of the mutant RyR2 protein. Thus, it is possible that the variable phenotypic expression observed in this large family may be due to the reduced expression of the G357S mutant protein. Future studies using patient-specific, induced pluripotent stem cell (iPSC) derived cardiomyocytes will be needed to test this possibility.

We have previously shown that CPVT mutations increase the propensity for SOICR as revealed by the increased fraction of cells that displayed SOICR. However, although the G357S mutation clearly affects the properties of SOICR (i.e. reducing the threshold for SOICR activation and termination, and increasing the fractional Ca²⁺ release), we did not observe an increase in the fraction of cells that displayed SOICR. This is likely due to the markedly reduced level of expression of the mutant protein. Since the occurrence of SOICR in HEK293 cells depends on the expression of RyR2 [21], the reduced level of RyR2 expression would decrease the occurrence of SOICR. Consistent with this view, indeed we observed a decreased maximum fraction of G357S expressing cells that exhibited SOICR. Therefore, the enhanced SOICR activity of the G357S mutant may be masked by its reduced expression when the SOICR activities were measured using a cell population-based assay. However, when the SOICR activities were measured in individual cells that displayed SOICR, it is clear that the

G357S mutation increases SOICR activity. On the other hand, the G357S mutation has no significant impact on the cytosolic Ca²⁺ activation of [³H]ryanodine binding or cytosolic Ca²⁺ induced fractional Ca²⁺ release in HEK293 cells, suggesting that the G357S mutation has little effect on cytosolic Ca²⁺-dependent activation of RyR2, which may also contribute to the variable disease expression in this family.

The mechanism by which the G357S mutation reduces the protein expression of RyR2 is likely intrinsic to the N-terminal region of RyR2. The mutation lies within a loop connecting two beta strands in a β -trefoil domain (domain B). In a high-resolution crystal structure of the RyR2 N-terminal region, the G357 backbone adopts a conformation that is only allowed for glycine residue. The G357S mutation would thus interfere with the folding of the G357 backbone. Indeed, the G357S mutation also results in decreased thermal stability of the N-terminal region of RyR2 (RyR2ABC only). The equivalent glycine appears close to an interface between the N-terminal domain (disease mutation hot spot 1) and the Central domain encompassing disease mutation hot spot 3 of RyR2 [1, 42, 43]. Importantly, the Central domain has recently been proposed to act as the transducer integrating conformational changes in the cytoplasmic assembly into the channel pore domain of RyR2 that controls the gating of the channel [42, 43, 48]. Hence, the interface between the N-terminal and Central domains may be required for normal allosteric coupling between the N-terminal region and the channel pore. As such, the G357S mutation may interfere with the coupling, explaining its effects on SOICR.

HEK293 cells have been widely used to study the impact of disease-associated RyR mutations on the intrinsic properties of the RyR channel. These studies have revealed important insights into the disease mechanisms of a number of RyR mutations. However, HEK293 cells lack many muscle-specific proteins. Thus, whether the intrinsic defects of the CPVT-linked G357S mutation in SOICR and RyR2 protein expression are manifested in cardiac cells has yet to be determined. Future studies using patient-specific, induced pluripotent stem cell (iPSC) derived cardiomyocytes or mouse models harboring the RyR2 G357S mutation will be needed to address this important question.

In summary, in the present study, we demonstrate that CPVT-associated RyR2 G357S mutation increases the SOICR activity by reducing the thresholds for SOICR activation and termination and increasing the fractional Ca²⁺ release. The G357S mutation also markedly reduces the protein expression of RyR2. The impact of the G357S mutation on both the SOICR activity and protein expression of RyR2 may contribute to the reduced penetrance of CPVT in this large family.

Acknowledgments

This work was supported by research grants from the Canadian Institutes of Health Research, the Heart and Stroke Foundation of Canada, the Canada Foundation for Innovation, and the Heart and Stroke Foundation Chair in Cardiovascular Research (to S.R.W.C.). Yingjie Liu is a recipient of the Alberta Innovates-Health Solutions (AIHS) Studentship Award. Jinhong Wei is a recipient of the Libin Cardiovascular Institute of Alberta and Cumming School of Medicine Postdoctoral Fellowship Award. Bo Sun is a recipient of the Heart and Stroke Foundation of Canada Junior Fellowship Award and the AIHS Fellowship Award. S.R. Wayne Chen is an AIHS Scientist.

Author Contributions

Conceptualization: Yingjie Liu, Jinhong Wei, Siobhan M. Wong King Yuen, Bo Sun, Yijun Tang, Ruiwu Wang, Filip Van Petegem, S. R. Wayne Chen.

Data curation: Yingjie Liu, Jinhong Wei, Siobhan M. Wong King Yuen, Bo Sun, Yijun Tang, Ruiwu Wang.

Formal analysis: Yingjie Liu, Jinhong Wei, Siobhan M. Wong King Yuen, Bo Sun, Yijun Tang, Ruiwu Wang, Filip Van Petegem, S. R. Wayne Chen.

Funding acquisition: Filip Van Petegem, S. R. Wayne Chen.

Investigation: Jinhong Wei.

Supervision: Filip Van Petegem, S. R. Wayne Chen.

Writing – original draft: Yingjie Liu, Ruiwu Wang, Filip Van Petegem, S. R. Wayne Chen.

Writing – review & editing: Yingjie Liu, Filip Van Petegem, S. R. Wayne Chen.

References

1. Priori S. G. and Chen S. R. (2011) Inherited dysfunction of sarcoplasmic reticulum Ca²⁺ handling and arrhythmogenesis. *Circulation research*. 108, 871–883 <https://doi.org/10.1161/CIRCRESAHA.110.226845> PMID: 21454795
2. Priori S. G., Napolitano C., Tiso N., Memmi M., Vignati G., Bloise R. et al. (2001) Mutations in the Cardiac Ryanodine Receptor Gene (hRyR2) Underlie Catecholaminergic Polymorphic Ventricular Tachycardia. *Circulation*. 103, 196–200. PMID: 11208676
3. Laitinen P. J., Brown K. M., Piippo K., Swan H., Devaney J. M., Brahmbhatt B. et al. (2001) Mutations of the cardiac ryanodine receptor (RyR2) gene in familial polymorphic ventricular tachycardia. *Circulation*. 103, 485–490 PMID: 11157710
4. Lahat H., Pras E., Olender T., Avidan N., Ben-Asher E., Man O. et al. (2001) A missense mutation in a highly conserved region of CASQ2 is associated with autosomal recessive catecholamine-induced polymorphic ventricular tachycardia in Bedouin families from Israel. *Am J Hum Genet*. 69, 1378–1184. <https://doi.org/10.1086/324565> PMID: 11704930
5. Postma A. V., Denjoy I., Hoorntje T. M., Lupoglazoff J. M., Da Costa A., Sebillon P. et al. (2002) Absence of Calsequestrin 2 Causes Severe Forms of Catecholaminergic Polymorphic Ventricular Tachycardia. *Circ Res*. 91, 21e–26
6. Roux-Buisson N., Cacheux M., Fourest-Lieuvain A., Fauconnier J., Brocard J., Denjoy I. et al. (2012) Absence of triadin, a protein of the calcium release complex, is responsible for cardiac arrhythmia with sudden death in human. *Human molecular genetics*. 21, 2759–2767 <https://doi.org/10.1093/hmg/dds104> PMID: 22422768
7. Nyegaard M., Overgaard M. T., Sondergaard M. T., Vranas M., Behr E. R., Hildebrandt L. L. et al. (2012) Mutations in calmodulin cause ventricular tachycardia and sudden cardiac death. *American Journal of Human Genetics*. 91, 703–712 <https://doi.org/10.1016/j.ajhg.2012.08.015> PMID: 23040497
8. Liu N., Colombi B., Memmi M., Zissimopoulos S., Rizzi N., Negri S. et al. (2006) Arrhythmogenesis in Catecholaminergic Polymorphic Ventricular Tachycardia: Insights From a RyR2 R4496C Knock-In Mouse Model. *Circ Res*. 99, 292–298 <https://doi.org/10.1161/01.RES.0000235869.50747.e1> PMID: 16825580
9. Paavola J., Viitasalo M., Laitinen-Forsblom P. J., Pasternack M., Swan H., Tikkanen I. et al. (2007) Mutant ryanodine receptors in catecholaminergic polymorphic ventricular tachycardia generate delayed afterdepolarizations due to increased propensity to Ca²⁺ waves. *European heart journal*. 28, 1135–1142 <https://doi.org/10.1093/eurheartj/ehl543> PMID: 17347175
10. Lakatta E. G. (1992) Functional implications of spontaneous sarcoplasmic reticulum Ca²⁺ release in the heart. *Cardiovasc Res*. 26, 193–214. PMID: 1423412
11. Marban E., Robinson S. W. and Wier W. G. (1986) Mechanisms of arrhythmogenic delayed and early afterdepolarizations in ferret ventricular muscle. *J Clin Invest*. 78, 1185–1192. <https://doi.org/10.1172/JCI112701> PMID: 3771791
12. Orchard C., Eisner D. and Allen D. (1983) Oscillations of intracellular Ca²⁺ in mammalian cardiac muscle. *Nature*. 304, 735–738 PMID: 6888540
13. Bassani J. W., Yuan W. and Bers D. M. (1995) Fractional SR Ca release is regulated by trigger Ca and SR Ca content in cardiac myocytes. *Am J Physiol*. 268, C1313–1319. PMID: 7762626
14. Diaz M. E., Trafford A. W., O'Neill S. C. and Eisner D. A. (1997) Measurement of sarcoplasmic reticulum Ca²⁺ content and sarcolemmal Ca²⁺ fluxes in isolated rat ventricular myocytes during spontaneous Ca²⁺ release. *The Journal of physiology*. 501 (Pt 1), 3–16

15. Shannon T. R., Pogwizd S. M. and Bers D. M. (2003) Elevated Sarcoplasmic Reticulum Ca²⁺ Leak in Intact Ventricular Myocytes From Rabbits in Heart Failure. *Circ Res.* 93, 592–594 <https://doi.org/10.1161/01.RES.0000093399.11734.B3> PMID: 12946948
16. Jiang D., Xiao B., Yang D., Wang R., Choi P., Zhang L. et al. (2004) RyR2 mutations linked to ventricular tachycardia and sudden death reduce the threshold for store-overload-induced Ca²⁺ release (SOICR). *Proc.Natl.Acad.Sci.U.S.A.* 101, 13062–13067 <https://doi.org/10.1073/pnas.0402388101> PMID: 15322274
17. Jiang D., Wang R., Xiao B., Kong H., Hunt D. J., Choi P. et al. (2005) Enhanced Store Overload-Induced Ca²⁺ Release and Channel Sensitivity to Luminal Ca²⁺ Activation Are Common Defects of RyR2 Mutations Linked to Ventricular Tachycardia and Sudden Death. *Circ Res.* 97, 1173–1181 <https://doi.org/10.1161/01.RES.0000192146.85173.4b> PMID: 16239587
18. Kannankeril P. J., Mitchell B. M., Goonasekera S. A., Chelu M. G., Zhang W., Sood S. et al. (2006) Mice with the R176Q cardiac ryanodine receptor mutation exhibit catecholamine-induced ventricular tachycardia and cardiomyopathy. *Proceedings of the National Academy of Sciences of the United States of America.* 103, 12179–12184 <https://doi.org/10.1073/pnas.0600268103> PMID: 16873551
19. Jones P. P., Jiang D., Bolstad J., Hunt D. J., Zhang L., Demareux N. et al. (2008) Endoplasmic reticulum Ca²⁺ measurements reveal that the cardiac ryanodine receptor mutations linked to cardiac arrhythmia and sudden death alter the threshold for store-overload-induced Ca²⁺ release. *The Biochemical journal.* 412, 171–178 <https://doi.org/10.1042/BJ20071287> PMID: 18092949
20. Sedej S., Heinzl F. R., Walther S., Dybkova N., Wakula P., Groborz J. et al. (2010) Na⁺-dependent SR Ca²⁺ overload induces arrhythmogenic events in mouse cardiomyocytes with a human CPVT mutation. *Cardiovascular research*
21. Tang Y., Tian X., Wang R., Fill M. and Chen S. R. (2012) Abnormal termination of Ca²⁺ release is a common defect of RyR2 mutations associated with cardiomyopathies. *Circulation research.* 110, 968–977 <https://doi.org/10.1161/CIRCRESAHA.111.256560> PMID: 22374134
22. Medeiros-Domingo A., Bhuiyan Z. A., Tester D. J., Hofman N., Bikker H., van Tintelen J. P. et al. (2009) The RYR2-encoded ryanodine receptor/calcium release channel in patients diagnosed previously with either catecholaminergic polymorphic ventricular tachycardia or genotype negative, exercise-induced long QT syndrome: a comprehensive open reading frame mutational analysis. *Journal of the American College of Cardiology.* 54, 2065–2074 <https://doi.org/10.1016/j.jacc.2009.08.022> PMID: 19926015
23. Bauce B., Rampazzo A., Basso C., Bagattin A., Daliento L., Tiso N. et al. (2002) Screening for ryanodine receptor type 2 mutations in families with effort-induced polymorphic ventricular arrhythmias and sudden death: early diagnosis of asymptomatic carriers. *Journal of the American College of Cardiology.* 40, 341–349 PMID: 12106942
24. Haugaa K. H., Leren I. S., Berge K. E., Bathen J., Loennechen J. P., Anfinson O. G. et al. (2010) High prevalence of exercise-induced arrhythmias in catecholaminergic polymorphic ventricular tachycardia mutation-positive family members diagnosed by cascade genetic screening. *Europace: European pacing, arrhythmias, and cardiac electrophysiology: journal of the working groups on cardiac pacing, arrhythmias, and cardiac cellular electrophysiology of the European Society of Cardiology.* 12, 417–423
25. Hayashi M., Denjoy I., Extramiana F., Maltret A., Buisson N. R., Lupoglazoff J. M. et al. (2009) Incidence and risk factors of arrhythmic events in catecholaminergic polymorphic ventricular tachycardia. *Circulation.* 119, 2426–2434 <https://doi.org/10.1161/CIRCULATIONAHA.108.829267> PMID: 19398665
26. van der Werf C., Nederend I., Hofman N., van Geloven N., Ebink C., Frohn-Mulder I. M. et al. (2012) Familial evaluation in catecholaminergic polymorphic ventricular tachycardia: disease penetrance and expression in cardiac ryanodine receptor mutation-carrying relatives. *Circulation.Arrhythmia and electrophysiology.* 5, 748–756 <https://doi.org/10.1161/CIRCEP.112.970517> PMID: 22787013
27. Wanguemert F., Bosch Calero C., Perez C., Campuzano O., Beltran-Alvarez P., Scornik F. S. et al. (2015) Clinical and molecular characterization of a cardiac ryanodine receptor founder mutation causing catecholaminergic polymorphic ventricular tachycardia. *Heart rhythm: the official journal of the Heart Rhythm Society.* 12, 1636–1643
28. Amador F. J., Liu S., Ishiyama N., Plevin M. J., Wilson A., MacLennan D. H. et al. (2009) Crystal structure of type I ryanodine receptor amino-terminal beta-trefoil domain reveals a disease-associated mutation "hot spot" loop. *Proceedings of the National Academy of Sciences of the United States of America.* 106, 11040–11044 <https://doi.org/10.1073/pnas.0905186106> PMID: 19541610
29. Lobo P. A. and Van Petegem F. (2009) Crystal structures of the N-terminal domains of cardiac and skeletal muscle ryanodine receptors: insights into disease mutations. *Structure (London, England: 1993).* 17, 1505–1514
30. Tung C. C., Lobo P. A., Kimlicka L. and Van Petegem F. (2010) The amino-terminal disease hotspot of ryanodine receptors forms a cytoplasmic vestibule. *Nature.* 468, 585–588 <https://doi.org/10.1038/nature09471> PMID: 21048710

31. Kimlicka L., Lau K., Tung C. C. and Van Petegem F. (2013) Disease mutations in the ryanodine receptor N-terminal region couple to a mobile intersubunit interface. *Nature communications*. 4, 1506 <https://doi.org/10.1038/ncomms2501> PMID: 23422674
32. Liu Y., Sun B., Xiao Z., Wang R., Guo W., Zhang J. Z. et al. (2015) Roles of the NH₂-terminal domains of cardiac ryanodine receptor in Ca²⁺ release activation and termination. *The Journal of biological chemistry*. 290, 7736–7746 <https://doi.org/10.1074/jbc.M114.618827> PMID: 25627681
33. Ho S. N., Hunt H. D., Horton R. M., Pullen J. K. and Pease L. R. (1989) Site-directed mutagenesis by overlap extension using the polymerase chain reaction [see comments]. *Gene*. 77, 51–59 PMID: 2744487
34. Zhao M., Li P., Li X., Zhang L., Winkfein R. J. and Chen S. R. (1999) Molecular identification of the ryanodine receptor pore-forming segment. *J Biol Chem*. 274, 25971–25974 PMID: 10473538
35. Laemmli U. K. (1970) Cleavage of structural proteins during the assembly of the head of bacteriophage T4. *Nature*. 227, 680–665. PMID: 5432063
36. Towbin H., Staehelin T. and Gordon J. (1979) Electrophoretic transfer of proteins from polyacrylamide gels to nitrocellulose sheets: procedure and some applications. *Proc Natl Acad Sci U S A*. 76, 4350–4434. PMID: 388439
37. Palmer A. E., Jin C., Reed J. C. and Tsien R. Y. (2004) Bcl-2-mediated alterations in endoplasmic reticulum Ca²⁺ analyzed with an improved genetically encoded fluorescent sensor. *Proceedings of the National Academy of Sciences of the United States of America*. 101, 17404–17409 <https://doi.org/10.1073/pnas.0408030101> PMID: 15585581
38. Tian X., Liu Y., Liu Y., Wang R., Wagenknecht T., Liu Z. et al. (2013) Ligand-dependent conformational changes in the clamp region of the cardiac ryanodine receptor. *The Journal of biological chemistry*. 288, 4066–4075 <https://doi.org/10.1074/jbc.M112.427864> PMID: 23258540
39. Li P. and Chen S. R. (2001) Molecular basis of ca(2)+ activation of the mouse cardiac ca(2)+ release channel (ryanodine receptor). *J Gen Physiol*. 118, 33–44. PMID: 11429443
40. Fabiato A. and Fabiato F. (1979) Calculator programs for computing the composition of the solutions containing multiple metals and ligands used for experiments in skinned muscle cells. *J Physiol (Paris)*. 75, 463–505
41. Kimlicka L., Tung C. C., Carlsson A. C., Lobo P. A., Yuchi Z. and Van Petegem F. (2013) The cardiac ryanodine receptor N-terminal region contains an anion binding site that is targeted by disease mutations. *Structure (London, England: 1993)*. 21, 1440–1449
42. Yan Z., Bai X. C., Yan C., Wu J., Li Z., Xie T. et al. (2015) Structure of the rabbit ryanodine receptor RyR1 at near-atomic resolution. *Nature*. 517, 50–55 <https://doi.org/10.1038/nature14063> PMID: 25517095
43. Peng W., Shen H., Wu J., Guo W., Pan X., Wang R. et al. (2016) Structural basis for the gating mechanism of the type 2 ryanodine receptor RyR2. *Science (New York, N.Y.)*
44. Priori S. G., Napolitano C., Memmi M., Colombi B., Drago F., Gasparini M. et al. (2002) Clinical and molecular characterization of patients with catecholaminergic polymorphic ventricular tachycardia. *Circulation*. 106, 69–74. PMID: 12093772
45. Tester D. J., Spoon D. B., Valdivia H. H., Makielski J. C. and Ackerman M. J. (2004) Targeted mutational analysis of the RyR2-encoded cardiac ryanodine receptor in sudden unexplained death: a molecular autopsy of 49 medical examiner/coroner's cases. *Mayo Clinic proceedings*. 79, 1380–1384 <https://doi.org/10.4065/79.11.1380> PMID: 15544015
46. Napolitano C. and Priori S. G. (2007) Diagnosis and treatment of catecholaminergic polymorphic ventricular tachycardia. *Heart rhythm: the official journal of the Heart Rhythm Society*. 4, 675–678
47. Roston T. M., Vinocur J. M., Maginot K. R., Mohammed S., Salerno J. C., Etheridge S. P. et al. (2015) Catecholaminergic polymorphic ventricular tachycardia in children: analysis of therapeutic strategies and outcomes from an international multicenter registry. *Circulation. Arrhythmia and electrophysiology*. 8, 633–642 <https://doi.org/10.1161/CIRCEP.114.002217> PMID: 25713214
48. Bai X. C., Yan Z., Wu J., Li Z. and Yan N. (2016) The Central domain of RyR1 is the transducer for long-range allosteric gating of channel opening. *Cell research*. 26, 995–1006 <https://doi.org/10.1038/cr.2016.89> PMID: 27468892